Thermopower and irreversibility field study of $Bi_{2-x}Pb_xSr_2Ca_2Cu_3O_{10+y}$

G. V. M. Williams,[1,2] J. L. Tallon,[2] and D. M. Pooke[2]
[1]*2. Physikalisches Institut, Universität Stuttgart, Pfaffenwaldring 57, D-70569 Stuttgart, Germany*
[2]*Industrial Research Limited, P.O. Box 31310, Lower Hutt, New Zealand*
(Received 22 December 1999)

We have used thermopower and magnetic irreversibility field measurements to probe the triple layer $Bi_{2-x}Pb_xSr_2Ca_2Cu_3O_{10+y}$ high-temperature superconducting cuprate. We find that the thermopower data can be analyzed in terms of a hole concentration deficit on the inner CuO_2 plane of $\delta p \sim 0.05$ when the outer CuO_2 planes are underdoped. However, this deficit does not appear to affect the magnetic irreversibility field H_{irr}, and it appears to be removed once the outer planes are optimally doped. We find that H_{irr} scales to a universal function, within the accessible hole concentration range, and that the maximum irreversibility field occurs at hole concentrations greater than those that can be achieved in this superconductor. We provide a simple model to account for the hole concentration dependence of the H_{irr} scaling prefactor in $Bi_{2-x}Pb_xSr_2Ca_2Cu_3O_{10+y}$ as well as in $Bi_2Sr_2CaCu_2O_{8+y}$ and $YBa_2Cu_3O_{7-y}$.

INTRODUCTION

The triple-layer $Bi_{2-x}Pb_xSr_2Ca_2Cu_3O_{10+y}$ high-temperature superconducting cuprate (HTSC) (Ref. 1) is currently the most useful for technological applications, however it is one of the least understood of all the HTSC's due to sample preparation difficulties. For example, this HTSC is synthesised from a $Bi_{2-x}Pb_xSr_2CaCu_2O_{8+y}$ precursor, and the incorporation of Pb is sensitive to annealing conditions, with consequences for impurity phase formation. It has also proved difficult to grow good-quality single crystals. The advantages of $Bi_{2-x}Pb_xSr_2Ca_2Cu_3O_{10+y}$ are its high-T_c value and its micaceous property that arises from the weak bonding between the BiO layers. This micaceous property is used to *c* axis align the superconductor by deformation-induced texturing within superconducting tapes and hence increase the superconducting critical current.

The understanding of the triple-layer $Bi_{2-x}Pb_xSr_2Ca_2Cu_3O_{10+y}$ (Bi-2223) HTSC is complicated by an inhomogeneous distribution of carriers between the three CuO_2 layers. Previous ^{17}O nuclear magnetic resonance (NMR) studies have shown that the inner CuO_2 layer can be significantly underdoped,[2,3] however, the distribution of holes over all three CuO_2 layers has not been systematically investigated as a function of hole concentration. Theoretical calculations have shown that the relative charge distribution in the three-layer HTSC can vary markedly with doping.[4]

One of the important parameters for characterizing HTSC is the magnetic irreversibility field, H_{irr}. The irreversibility field is defined as the magnetic field at which $M(H)$ becomes reversible and independent of the previous path. While there are a number of conflicting models to describe the magnetic irreversibility field, it is clear that the higher H_{irr} values are associated with higher superconducting critical currents. In particular, it has been shown for the double CuO_2 layer HTSC $Y_{0.8}Ca_{0.2}Ba_2Cu_3O_{7-y}$ that the irreversibility temperature is correlated with the superconducting critical current and that both reach a maximum near an overdoped hole concentration of $p=0.19$.[5]

In this paper, we report room-temperature thermopower and variable-temperature magnetic irreversibility field measurements on Bi-2223. The irreversibility measurements were performed on the same polycrystalline sample, which allows intrinsic effects to be measured. We use a polycrystalline sample rather than a single crystal because polycrystalline HTSC are being used in technological applications and, as mentioned above, it is not yet possible to make good-quality single crystals. We show that the room-temperature thermopower can be modeled in terms of a hole concentration deficit on the middle CuO_2 layer, compatible with ^{17}O NMR measurements, and the irreversibility field increases monotonically in magnitude with increasing hole concentration and scales to a universal curve over the accessible hole concentration range. We show that the H_{irr} data favors either the three-dimensional (3D) vortex lattice melting or the 3D-2D flux-line transition models. In particular we show that these models can account for the hole concentration dependence of the H_{irr} scaling prefactor in Bi-2223 as well as in $Bi_2Sr_2CaCu_2O_{8+y}$ (Bi-2212) and $YBa_2Cu_3O_{7-y}$.

EXPERIMENTAL DETAILS

Polycrystalline $Bi_{2-x}Pb_xSr_2Ca_2Cu_3O_{10+y}$ samples, with $x=0.34$, were prepared by standard solid-state techniques; pellets were ground and repressed several times during the sintering process to achieve phase uniformity, and sintering was carried out in crucibles with close-fitting lids to avoid Pb loss. The hole concentration, and hence T_c, was altered by annealing the samples at different temperatures and oxygen partial pressures as described elsewhere.[6]

Magnetization measurements were performed using a vibrating-sample magnetometer over temperatures ranging from 40 to 120 K. The measurements were performed on the same sample where the hole concentration was altered by annealing at different temperatures and oxygen partial pressures followed by quenching into liquid nitrogen. The irreversibility field was obtained from $M(H)$ plots at fixed temperatures and was defined as the magnetic field at which the difference between M for increasing and decreasing fields fell to less than 0.02 emu/cm^3. The room-temperature ther-

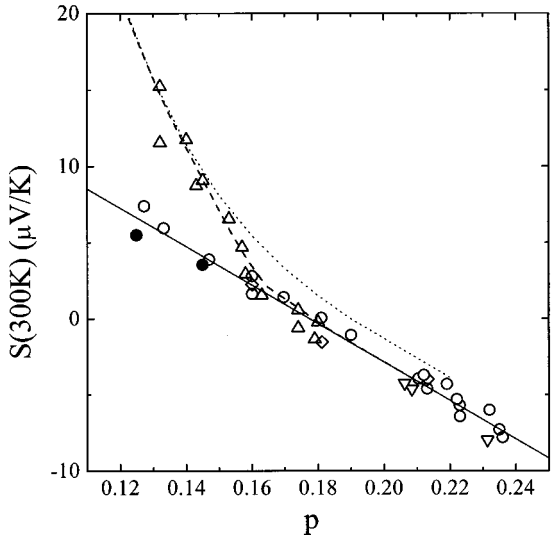

FIG. 1. Plot of the room-temperature thermopower, $S(300\,\mathrm{K})$, against hole concentration p for Bi-2223 (open up triangles), Bi-2212 (open circles), Tl-1212 (open diamonds) (Ref. 8), Tl-2201 (open down triangles) (Ref. 8), and Tl-2223 (filled circles) (Ref. 8) HTSC. The solid line is a best fit to the data excluding Bi-2223. The dashed curve is the model described in the text with an inner CuO_2 plane hole concentration deficit of $\delta p = \delta p_0/2[1-\tanh((p-0.16)/0.01)]$ and the dotted line is the model described in the text with an inner CuO_2 plane hole concentration deficit of $\delta p = 0.05$.

mopower, $S(300\,\mathrm{K})$, was measured using a technique described previously.[7]

RESULTS AND ANALYSIS

It is apparent in Fig. 1 that the doping dependence of $S(300\,\mathrm{K})$ for Bi-2223 follows a curve different from that of other HTSC's. Here we plot the thermopower data against hole concentration for Bi-2223 (open up triangles), Bi-2212 (open circles), Tl-1212 (open diamonds) (Ref. 8) and Tl-2201 (open down triangles) (Ref. 8) samples. The hole concentration was estimated from the superconducting transition temperature, T_c, using the empirical relation $T_c = T_{c0}[1-82.6(p-0.16)^2]$ which has been shown to apply for these HTSC.[9] Only the Bi-2223 samples do not follow the common curve found by Obertelli *et al.*[8] for a variety of HTSC's. We show that this departure cannot be simply attributed to the existence of three CuO_2 layers by including data from the triple layer Tl-2223 HTSC (filled circles).[8] This fits the correlation well.

A possible explanation for the departure of the Bi-2223 room-temperature thermopower from the common $S(300\,\mathrm{K},p)$ curve is an unequal distribution of holes on the three CuO_2 planes. This explanation has been used to account for the extra peaks in the ^{17}O NMR spectra from Bi-2223 samples.[2,3] However, these measurements were not performed as a function of hole concentration. By comparing the ^{17}O NMR shift of the peaks in Bi-2223 samples[2] with the ^{89}Y NMR shift in $Y_{0.8}Ca_{0.2}Ba_2Cu_3O_{7-y}$ (Ref. 10) and using the known hyperfine coupling constants[11] it is possible to estimate that the inner CuO_2 plane had a hole deficit of $\delta p \sim 0.06$ relative to the outer layers.

We show below that it is also possible to analyze $S(300\,\mathrm{K},p)$ from Bi-2223 in terms of a similar hole concentration deficit on the inner CuO_2 layer when the sample is underdoped. For higher doping levels the deficit appears to reduce to zero. The occurrence of an inhomogeneous distribution over the two inequivalent CuO_2 planes raises the question as to how to define the overall doping state. We assume that T_c is governed by the doping state of the two outer layers and deduce the quoted values of p for these layers. We start by noting that the conduction is quasi-2D and hence it is reasonable to model the thermopower as

$$S(p) = S(p)\frac{2\sigma(p)}{2\sigma(p)+\sigma(p-\delta p)} + S(p-\delta p)\frac{\sigma(p-\delta p)}{2\sigma(p)+\sigma(p-\delta p)}, \quad (1)$$

where σ is the electrical conductivity and the total average hole concentration is $p-\delta p/3$. The first term is the contribution from the two outer CuO_2 layers while the second term is the contribution from the hole-deficient inner CuO_2 layer. As there is no systematic *ab*-plane conductivity data on Bi-2223, we approximate $\sigma(p)$ as $\sigma(p) \propto p$ for each layer. This approximation is valid in Bi-2212 over a similar hole concentration range.[12] We model the data with $S(300\,\mathrm{K},p)$ being linear for $p > 0.12$ and $S(p) = 992\exp(-38.1p)$ for $p < 0.12$ as observed in other HTSC's.[8] It can be seen by the dotted curve in Fig. 1 that a constant δp of 0.05 can describe the data for $p < 0.16$ but the predicted thermopower values are too large for $p > 0.16$. A better representation of the data can be obtained by assuming a p-dependent deficit. We show by the dashed curve in Fig. 1 that a simple model using $\delta p = (\delta p_0/2)[1-\tanh((p-0.16)/0.01)]$ can statisfactorily describe the data with $\delta p_0 = 0.05$. Later, we will see that a p-dependent deficit has no significant effect on the magnetic irreversibility field H_{irr}.

We now consider the magnetic irreversibility field. It can be seen in Fig. 2(a) that H_{irr} for Bi-2223 is progressively larger for higher hole concentrations. Here we plot H_{irr} against temperature, normalized by the superconducting transition temperature, in order of doping: $T_c = 107.2\,\mathrm{K}$ (open squares, overdoped), $T_c = 108.9\,\mathrm{K}$ (open up triangles, overdoped), $T_c = 108.6\,\mathrm{K}$ (open circles, underdoped), $T_c = 107.1\,\mathrm{K}$ (open down triangles, underdoped), $T_c = 105.3\,\mathrm{K}$ (open diamonds, underdoped) and $T_c = 101.7\,\mathrm{K}$ (stars, underdoped). The effect of different hole concentrations is clearer in Fig. 3 where we plot the p dependence of H_{irr} when $T/T_c = 0.8$ (open circles, left axis). For comparison, we also show T_c (filled circles, right axis) and the $T_c(p)$ universal curve (solid curve, right axis).[9] Notably, H_{irr} continues to increase even for hole concentrations greater than optimal doping ($p = 0.16$). It is also important to show that even at a fixed temperature the value of H_{irr} is increasing with hole concentration. This is apparent in Fig. 3 where we also plot H_{irr} against hole concentration for $T = 87\,\mathrm{K}$ (open up triangles). This temperature is arbitrarily chosen as the temperature at which $T/T_c = 0.8$ for the sample with the highest T_c.

We show in Fig. 2(b) that H_{irr} for these different doping levels scales to a universal curve of the form $H_{\mathrm{irr}} = H_{\mathrm{irr}}(p) f(T/T_c)$. A similar scaling has been observed in

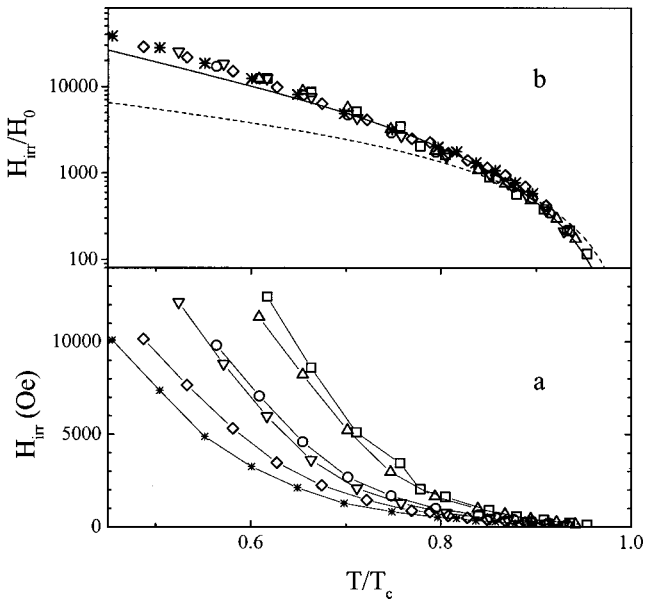

FIG. 2. (a) Plot of the magnetic irreversibility field H_{irr} against the reduced temperature, T/T_c, for Bi-2223 when $T_c=107.2$ K (open squares), $T_c=108.9$ K (open up triangles), $T_c=108.6$ K (open circles), $T_c=107.1$ K (open down triangles), $T_c=105.3$ K (open diamonds) and $T_c=101.7$ K (*). (b) Plot of the same data as in (a) scaled onto a common curve. The solid curve is H_{irr} calculated in the 3D vortex lattice melting model and the dashed curve is H_{irr} calculated in the 3D-2D flux-line transition model.

$Y_{0.8}Ca_{0.2}BaCu_3O_{7-y}$,[13] $YBa_2Cu_3O_{7-y}$,[14] and in $Y_{1-x}Pr_xBa_2Cu_3O_{7-y}$.[15] The scaling parameter, $H_{irr}(p)$, is plotted in Fig. 4 for Bi-2223 (filled circles), $YBa_2Cu_3O_{7-y}$ (open circles[14]) and Bi-2212 (open squares[16]). Also plotted is the scaling field, H^*, for the entire vortex phase diagram found by Blasius *et al.*[17] for Bi-2212 (open diamonds). It is clear that $H_{irr}(p)$ for all these HTSC's and Bi-2223 follow a similar hole concentration dependence. Therefore the anisotropic distribution of holes over the three CuO_2 planes in Bi-2223 seems to have no significant effect on $H_{irr}(p)$. Presumably, H_{irr} is dominated rather by coupling across the $Sr_2Bi_2O_4$ block layer than within the CuO_2 trilayer. This figure suggests that the maximum $H_{irr}(p)$ in Bi-2223 lies well beyond the currently-achievable maximum hole concentration.

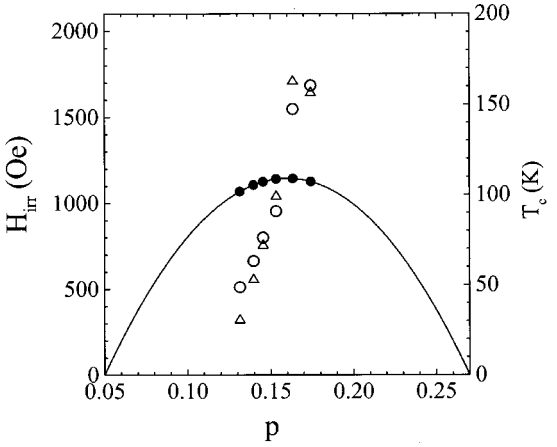

FIG. 3. Plot of H_{irr} against hole concentration when $T/T_c=0.8$ (open circles) and $T=87$ K (open up triangles) for a $Bi_{2-x}Pb_xSr_2Ca_2Cu_3O_{10+y}$ HTSC. Also shown is T_c against hole concentration (filled circles) and the universal $T_c(p)$ curve (Ref. 9).

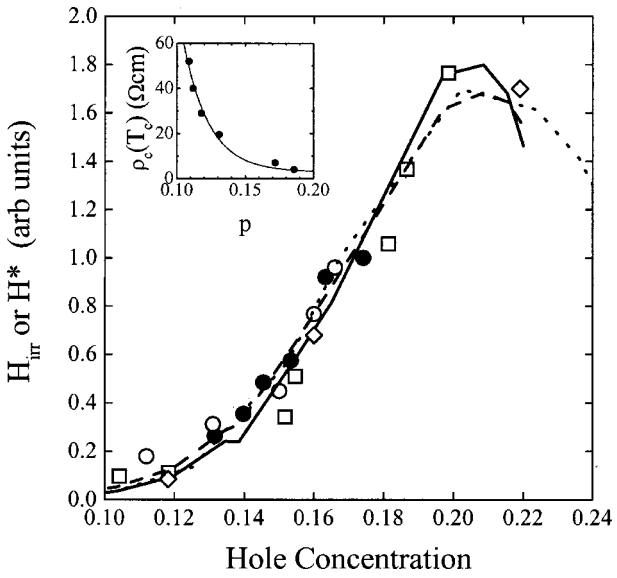

FIG. 4. Plot of the magnetic irreversibility field scaling factor, $H_{irr}(p)$, against hole concentration for Bi-2223 (filled circles). The data are normalized by $H_{irr}(p)$ for the most overdoped sample. Also included is $H_{irr}(p)$ for $YBa_2Cu_3O_{7-y}$ [open circles (Ref. 14)] and for Bi-2212 [open squares (Ref. 16)]. Data for the scaling field H^* for the vortex phase diagram of Bi-2212 including the irreversibility field is shown by open diamonds (Ref. 17). The data for Bi-2212 and $YBa_2Cu_3O_{7-y}$ are normalized to fall on the common curve. The curves are calculations of H_{irr} as described in the text using the ρ_c data of Watanabe *et al.* (Ref. 12) and the λ_{ab}^{-2} data from $Y_{0.8}Ca_{0.2}BaCu_3O_{7-y}$ (Ref. 29) [3D vortex lattice melting model (solid curve) and 3D-2D flux-line transition model (dashed curve)] and $Tl_{0.5+x}Pb_{0.5-x}Sr_2Ca_{1-y}Y_yCu_2O_7$ (Ref. 30) [3D vortex lattice melting model (dotted curve)]. Inset: Plot of the Bi-2212 *c*-axis resistivity at T_c (Ref. 12). The solid curve is the ρ_c curve used to model the $H_{irr}(p)$ data.

Of course we are considering here the irreversibility field as a universal function of T/T_c and in these more heavily overdoped samples T_c is falling rapidly. The optimal doping state for maximum irreversibility field at a fixed *absolute* temperature therefore lies at a lower doping state than the maximum shown in Fig. 4. In this respect it is more convenient to consider the irreversibility temperature $T_{irr}(H,p)$ at a fixed field. Elsewhere[5] it was shown that $T_{irr}(5\text{ T},p)$, as well as the low-temperature critical current, J_c, both pass through a sharp maximum at $p\sim0.19$ for $Y_{0.8}Ca_{0.2}Ba_2Cu_3O_{7-y}$. This critical doping state $p\sim0.19$ coincides with the disappearance of the pseudogap and the occurrence of associated maxima in both the superfluid density and condensate density for all HTSC's.[5] We thus also expect an improvement in J_c and $T_{irr}(H,p)$ for Bi-2223 if the hole concentration could be increased to ~0.19 in this material.

In seeking to understand the $H_{irr}(T/T_c)$ scaling curve in Fig. 2(b) we note that there is no consensus concerning the origin and modeling of $H_{irr}(T)$. A number of conflicting models have been used to analyze H_{irr} including; (i) a fluctuation-induced 3D-2D flux-line transition involving the decoupling of vortices to independent 2D lattices,[13,17] (ii) 3D

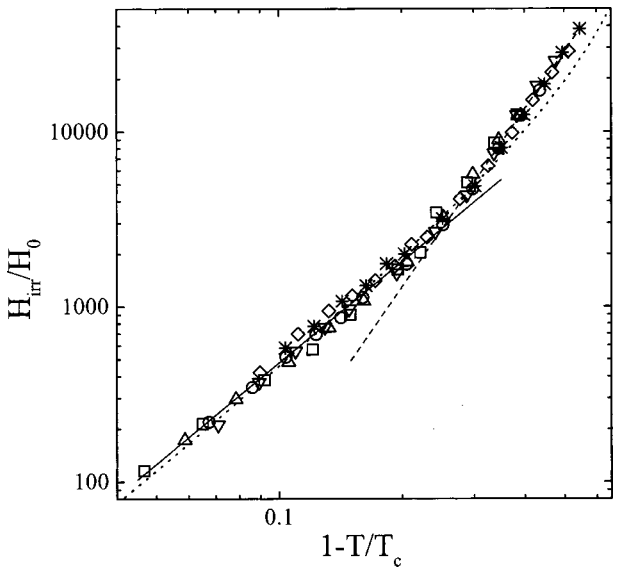

FIG. 5. Plot of the scaled $\log_{10}(H_{\rm irr})$ against $\log_{10}(1-T/T_c)$ for Bi-2223. Also shown is fits to $(1-T/T_c)^n$ with $n=1.92$ (solid line) and $n=3.37$ (dashed line). The dotted curve is $H_{\rm irr}$ calculated in the 3D vortex lattice melting model.

vortex lattice melting related to a vanishing vortex shear modulus,[18,19] (iii) flux-line pinning or flux creep,[14] and (iv) surface or geometric effects.[20] The relevant regimes may shift with doping, temperature and field strength.[15] Most models predict critical behavior near T_c. For this reason we plot $\log_{10}(H_{\rm irr}(t))$ against $\log_{10}(1-t)$ in Fig. 5 where $t=T/T_c$. The data can be described by $H_{\rm irr}\propto(1-t)^n$ with $n=1.92$ for $t>0.75$ and $n=3.37$ for $t<0.75$. The exponent for $t>0.75$ is close to that found by Kopelevich *et al.* ($n=2$) (Ref. 19) from a study on a Bi-2223 sample with $T_c=109$ K and for $t>0.8$. Kopelevich *et al.* noted that n was larger (>4) for $t<0.8$. An exponent of $n=2$ was found in a study on Bi-2212 by Schilling *et al.*[18] for $t>0.8$. In these studies the exponent of $n=2$ near T_c was used to argue that $H_{\rm irr}$ arises from 3D vortex lattice melting. However, a study by Almasan *et al.*[15] on $Y_{1-x}Pr_xBa_2Cu_3O_{7-y}$ found a different exponent of $n=1.5$ near T_c while Ossandon *et al.*[14] found an exponent of 1.7 from a study on $YBa_2Cu_3O_{7-y}$. The different experimental exponents ranging from $n=1.5$ to $n=2$ indicate that it is not possible to use the exponent alone to deduce which of the models mentioned earlier can best describe $H_{\rm irr}$.

While it is an open question in the literature as to the origin of $H_{\rm irr}$, we believe that the experimental evidence favors either the 3D-2D flux-line transition model or the 3D vortex lattice melting model. We show below that the 3D vortex lattice melting model can describe the Bi-2233 $H_{\rm irr}$ temperature dependence near T_c and both the 3D vortex lattice melting model and the 3D-2D flux-line transition model can account for the exponential dependence of $H_{\rm irr}$ on the distance between each CuO block layers. Furthermore, these two models can equally account for the hole concentration dependence of the $H_{\rm irr}$ scaling prefactor.

We first consider the temperature dependence of $H_{\rm irr}$ within the 3D-2D flux-line transition and the 3D vortex lattice melting models. It has previously been shown that $H_{\rm irr}\propto\lambda_{ab}^{-3}\gamma^{-2}T^{-1}$ for the 3D-2D flux-line transition model[21] and $H_{\rm irr}\propto\lambda_{ab}^{-4}\gamma^{-2}T^{-2}$ for the 3D vortex lattice melting model[21] where $\gamma(=\lambda_c/\lambda_{ab})$ is the penetration depth anisotropy. It is assumed that γ is temperature independent[18,21] and that $\lambda_{ab}^{-2}\propto\lambda_{ab}^{-2}(0)(1-t)$. These assumptions lead to $H_{\rm irr}\propto\lambda_{ab}(0)^{-3}\gamma^{-2}(1-t)^{1.5}t^{-1}$ for the 3D-2D flux-line transition model and $H_{\rm irr}\propto\lambda_{ab}(0)^{-4}\gamma^{-2}(1-t)^2t^{-2}$ for the 3D vortex lattice melting model. However, there is evidence that γ is temperature dependent. It has been found that λ_c can be described within the Josephson coupling model by[22]

$$\lambda_c^{-2}\propto\frac{\Delta'}{\rho_c}\tanh\left(\frac{\Delta'}{2k_BT}\right).$$

It is also important to note that, even if the temperature dependence of γ is ignored, fitting $H_{\rm irr}$ to $(1-t)^n$ (i.e., ignoring the t^{-1} or t^{-2} factors) will lead to $n=1.66$ for the 3D-2D flux-line transition model and $n=2.35$ for the 3D vortex lattice melting model when $t>0.8$ rather than $n=1.5$ and $n=2.0$, respectively.

Including the effect of the temperature dependence of γ within the BCS model will lead to $H_{\rm irr}$ of the form

$$H_{\rm irr}\propto\frac{\Delta'(0)}{T_c}\lambda_{ab}(0)^{-1}\rho_c^{-1}\tanh\left(\frac{\Delta'(0)}{2k_BT_c}\frac{g(t)}{t}\right)\frac{g(t)\sqrt{f(t)}}{t} \tag{2}$$

for the 3D-2D flux-line transition model,

$$H_{\rm irr}\propto\frac{\Delta'(0)}{T_c}\lambda_{ab}(0)^{-2}\rho_c^{-1}T_c^{-1}\tanh\left(\frac{\Delta'(0)}{2k_BT_c}\frac{g(t)}{t}\right)\frac{g(t)f(t)}{t^2} \tag{3}$$

for the 3D vortex melting model where $\Delta'(T)=\Delta'(0)g(t)$, $\Delta'(T)$ is the superconducting order parameter [to be distinguished from the superconducting spectral gap, $\Delta(T)$] and $\lambda_{ab}(T)^{-2}=\lambda_{ab}(0)^{-2}f(t)$. It is possible to show by calculating $\Delta'(T)$ and $\lambda_{ab}(T)^{-2}$ within the BCS model and using a *d*-wave superconducting order parameter that $H_{\rm irr}$ can be approximated by $(1-t)^n$ with $n=1.45$ for the 3D-2D flux-line transition model and $n\sim2.08$ for the 3D vortex lattice melting model when $t>0.8$. We show in Fig. 2 that the 3D vortex lattice melting model (solid curve) does give a better representation of the data than the 3D-2D flux-line transition model (dashed curve) near T_c. This is clearer in Fig. 5 where $H_{\rm irr}$ is also plotted for the 3D vortex lattice melting model (dotted curve). Care must be taken in drawing the conclusion that this provides conclusive evidence that $H_{\rm irr}$ arises from 3D vortex lattice melting. This is because the BCS temperature dependence of $f(t)$ near T_c is not universally observed in the HTSC, possibly due to inhomogeneity, fluctuations or a finite cutoff in the expansion of the superconducting order parameter Δ'.[23–25] This can alter the temperature dependence of $H_{\rm irr}$ near T_c.

We now consider the dependence of $H_{\rm irr}$ on the block layer spacing d_b defined as the spacing between the CuO_2 layer blocks. We have previously found that $H_{\rm irr}(t=0.75,p=0.16)$ increases exponentially with decreasing d_b.[13] This can be accounted for by both the 3D-2D flux-line transition model and the 3D vortex lattice melting model. For both of these models the exponential dependence of $H_{\rm irr}(t=0.75,p=0.16)$ on d_b arises from the dependence on ρ_c. It can easily be shown in a simple superconductor-insulator-

superconductor tunneling junction that $\rho_c \propto \exp(-d_b/d_0)$ where d_0 is proportional to the wave function penetration into the insulating barrier. Thus, from Eqs. (2) and (3) it is apparent that $H_{\rm irr}(t=0.75,p=0.16) \propto \exp(d_b/d_0)$. It should be noted that, experimentally, d_0 is small with a value of 0.19 nm. This can be compared with d_b which ranges from 0.4 to 1.2 nm. It is difficult to see how the other models could account for the exponential dependence of $H_{\rm irr}(t=0.75,p=0.16)$ on d_b, which increases by a factor of $\sim$70 in going from Bi-2223 to $YBa_2Cu_3O_{7-y}$.[13] For example, in one derivation of the flux-line pinning[14] $H_{\rm irr}$ has been found to follow $H_{\rm irr} \propto \lambda_{ab}(0)^{-1} U(0)^{1/2} (1-t)^{1.7}$ for $YBa_2Cu_3O_{7-y}$ where U is the superconducting condensation energy. Using $U_0 = 30$ J/mol and $\lambda_{ab} = 160$ nm for Bi-2212 at optimal doping,[26] it is possible to show that this flux-line pinning model would predict an increase in $H_{\rm irr}(t=0.75,p=0.16)$ of $\sim$2 when going from Bi-2212 to $YBa_2Cu_3O_{7-y}$ compared with the observed value of $\sim$70. It is also difficult to see how surface effects (dominated by U_0 which is largely independent of anisotropy) could account for such a large increase especially as it has recently been shown that vortex motion is governed by bulk effects rather than surface barriers.[27]

We show in Fig. 4 that the hole concentration dependence of $H_{\rm irr}(p)$ from Bi-2223, Bi-2212, and $YBa_2Cu_3O_{7-y}$ can be explained by the 3D vortex lattice melting model (solid curve) or the 3D-2D flux-line transition model (dashed curve) where from Eqs. (2) and (3),

$$H_{\rm irr}(p) \propto \frac{\Delta'(0)}{T_c} \lambda_{ab}(0)^{-2} T_c^{-1} \rho_c^{-1} \quad \text{or}$$

$$H_{\rm irr}(p) \propto \frac{\Delta'(0)}{T_c} \lambda_{ab}(0)^{-1} \rho_c^{-1},$$

respectively. The basic features of this interpretation are that $H_{\rm irr}(p)$ is dominated by the appearance of a maximum in the superfluid density $[\sim \lambda_{ab}(0)^{-2}]$ at $p=0.19$ and by the strong p dependence of ρ_c for $p \leqslant 0.19$. Noting that Δ' is the order parameter, the factor $\Delta'(0)/T_c$ is assumed to remain constant, independent of doping. The ratio of the spectral gap to T_c, $\Delta(0)/T_c$ is found from heat capacity to remain constant ($\sim$2.9) on the overdoped side but rises rapidly around optimal doping with the opening of the pseudogap. In the presence of a normal-state pseudogap with the same angular variation in k space as Δ', the relationship between the spectral gap and the order parameter may be modeled as $\Delta(0)^2 = \Delta'(0)^2 + E_g^2$.[28] To a reasonable approximation T_c will scale as $\Delta'(0)$. Thus $H_{\rm irr}(p) \propto \lambda_{ab}(0)^{-2} T_c^{-1} \rho_c^{-1}$ for the 3D vortex lattice melting model and $H_{\rm irr}(p) \propto \lambda_{ab}(0)^{-1} \rho_c^{-1}$ for the 3D-2D flux-line transition model. In the absence of data for Bi-2223 we estimate ρ_c from a previous study on Bi-2212 single crystals.[12] The c-axis resistivity at T_c, shown in the inset to Fig. 4, decreases dramatically with increasing hole concentration. We obtain a functional form for ρ_c by fitting this data to a constant plus an exponential as shown by the solid curve in the inset to Fig. 4. The p dependence of $\lambda_{ab}(0)^{-2}$ has been measured by μSR for $Y_{0.8}Ca_{0.2}BaCu_3O_{7-y}$ (Ref. 29) and we plot the variation of $H_{\rm irr}$ in Fig. 4 for the 3D vortex lattice melting model (solid curve) and for the 3D-2D flux-line transition model (dashed curve). The fit to the experimental data for both models is quite reasonable. The dotted curve shows the same calculation of $H_{\rm irr}$ for the 3D vortex lattice melting model using $\lambda_{ab}(0)^{-2}$ measured from samples of $Tl_{0.5+x}Pb_{0.5-x}Sr_2Ca_{1-y}Y_yCu_2O_7$.[30] For this compound, the variation in $\lambda_{ab}(0)^{-2}$ with doping is very similar to that found for $Y_{0.8}Ca_{0.2}Ba_2Cu_3O_{7-y}$ and the common behavior is believed to be generic and therefore applicable to Bi-2223. The curves for $H_{\rm irr}(p)$ shown in Fig. 4 follow the data very well across the measured doping range. Interestingly, they indicate that $H_{\rm irr}(p)$ saturate for $p > 0.2$. We note tentatively that the combination of Bi-2212 data (squares[16] and diamonds[17]) do appear to support the occurrence of this saturation.

CONCLUSIONS

In conclusion, we find that the room-temperature thermopower of Bi-2223 can be interpreted in terms of a hole concentration deficiency on the inner CuO_2 layer for underdoped samples. However, for overdoped samples the data can be analyzed in terms of a uniform distribution of holes over all three CuO_2 planes. We also find that $H_{\rm irr}(T)$ can be scaled onto a common curve. Both $H_{\rm irr}(T)$ and the scaling prefactor, $H_{\rm irr}(p)$, systematically increase with increasing hole concentration. By comparing $H_{\rm irr}(p)$ in Bi-2223 with the values found in $YBaCu_3O_{7-y}$ and Bi-2212 it is found that the maximum $H_{\rm irr}(p)$ in Bi-2223 is beyond currently achievable hole concentrations. We provide a simple interpretation of $H_{\rm irr}(p)$ for Bi-2223, as well as for Bi-2212 and $YBaCu_3O_{7-y}$, using the 3D vortex melting model or 3D-2D flux-line transition model where ρ_c^{-1} dominates $H_{\rm irr}(p)$ for $p < 0.19$ and $\lambda_{ab}(0)^{-2}$ dominates for $p > 0.19$.

ACKNOWLEDGMENTS

We acknowledge funding support from the New Zealand Foundation for Research Science and Technology, the Royal Society of New Zealand (J.L.T.), and the Alexander von Humboldt Foundation (G.V.M.W.).

[1] J. L. Tallon, R. G. Buckley, P. W. Gilberd, M. R. Presland, I. W. M. Brown, M. E. Bowden, L. A. Christian, and R. Goguel, Nature (London) **333**, 153 (1988).

[2] R. Dupree, Z. P. Han, A. P. Howes, D. M. Paul, M. E. Smith, and S. Male, Physica C **175**, 269 (1991).

[3] A. Trokiner, L. Le. Noc, J. Schneck, A. M. Pougnet, R. Mellet, J. Primot, H. Savary, Y. M. Gao, and S. Aubry, Phys. Rev. B **44**, 2426 (1991).

[4] E. M. Haines and J. L. Tallon, Phys. Rev. B **45**, 3172 (1992).

[5] J. L. Tallon, J. W. Loram, G. V. M. Williams, J. R. Cooper, I. R. Fisher, and C. Bernhard, Phys. Status Solidi B **215**, 531 (1999).

[6] G. V. M. Williams, D. M. Pooke, D. J. Pringle, H. J. Trodahl, J.

L. Tallon, J. Quilty, N. Malde, J. L. Macmanus-Driscoll, A. Crossley, and L. F. Cohen, Phys. Rev. B **62**, 1379 (2000).
[7] G. V. M. Williams, J. L. Tallon, R. Meinhold, and A. Janossy, Phys. Rev. B **51**, 16 503 (1995).
[8] S. D. Obertelli, J. R. Cooper, and J. L. Tallon, Phys. Rev. B **46**, 14 928 (1992).
[9] M. R. Presland, J. L. Tallon, R. G. Buckley, R. S. Liu, and N. E. Flower, Physica C **176**, 95 (1991).
[10] G. V. M. Williams and J. L. Tallon, Phys. Rev. B **57**, 10 984 (1998).
[11] M. Mehring, Appl. Magn. Reson. **3**, 383 (1992).
[12] T. Watanabe, T. Fujii, and A. Matsuda, Phys. Rev. Lett. **79**, 2113 (1997).
[13] J. L. Tallon, G. V. M. Williams, C. Bernhard, D. M. Pooke, M. P. Staines, J. D. Johnson, and R. H. Meinhold, Phys. Rev. B **53**, 11 972 (1996).
[14] J. G. Ossandon, J. R. Thompson, D. K. Cristen, B. C. Sales, H. R. Kerchner, J. O. Thomson, Y. R. Sun, K. W. Lay, and J. E. Tkaczyk, Phys. Rev. B **45**, 12 534 (1992).
[15] C. C. Almasan, M. C. de Andrade, Y. Dalichaouch, J. J. Neumeier, C. L. Seaman, M. B. Maple, R. P. Guertin, M. V. Kuric, and J. C. Garland, Phys. Rev. Lett. **69**, 3812 (1992).
[16] K. Kishio, J. Shimoyama, Y. Kotaka, and K. Yamafuji, *Critical Currents in Superconductors*, edited by H. W. Weber (World Scientific, Singapore, 1994), p. 339.
[17] T. Blasius, Ch. Niedermayer, J. L. Tallon, D. M. Pooke, A. Golnik, and C. Bernhard, Phys. Rev. Lett. **82**, 4926 (1999).
[18] A. Schilling, R. Jin, J. D. Guo, and H. R. Ott, Phys. Rev. Lett. **71**, 1899 (1993).
[19] Y. Kopelevich, S. Moehlecke, and J. H. S. Torres, Phys. Rev. B **49**, 1495 (1994).
[20] D. Majer, E. Zeldov and M. Konczykowski, Phys. Rev. Lett. **75**, 1166 (1995).
[21] V. Hardy, Physica C **232**, 347 (1994).
[22] T. Shibauchi, H. Kitano, K. Uchinokura, A. Maeda, T. Kimura, and K. Kishio, Phys. Rev. Lett. **72**, 2263 (1994).
[23] T. Jacobs, S. Sridhar, Qiang Li, G. D. Gu, and N. Koshizuka, Phys. Rev. Lett. **75**, 4516 (1995).
[24] Shih-Fu Lee, D. C. Morgan, R. J. Ormeno, D. M. Broun, R. A. Doyle, J. R. Waldram, and K. Kadowaki, Phys. Rev. Lett. **77**, 735 (1996).
[25] E. Schachinger, J. P. Carbotte, and F. Marsiglio, Phys. Rev. B **56**, 2738 (1997).
[26] J. L. Tallon, Phys. Rev. B **58**, 5956 (1998).
[27] A. Mazilu, H. Safar, D. López, W. K. Kwok, G. W. Crabtree, P. Guptasarma, and D. G. Hinks, Phys. Rev. B **58**, 8913 (1998).
[28] J. W. Loram, K. A. Mirza, J. R. Cooper, and W. Y. Liang, J. Supercond. **7**, 243 (1994).
[29] C. Bernhard, Ch. Niedermayer, U. Binninger, A. Hofer, Ch. Wenger, J. L. Tallon, G. V. M. Williams, E. J. Ansaldo, J. I. Budnick, C. E. Stronach, D. R. Noakes, and M. A. Blankson-Mills, Phys. Rev. B **52**, 10 488 (1995).
[30] C. Bernhard, J. L. Tallon, T. Blasius, A. Golnick, and Ch. Niedermayer, Phys. Rev. B (to be published).